

given that photoexcitation of coordination compounds, which undergo very small isotropic changes (0.01 Å) in their van der Waals radii, produces reaction volume changes readily detectible by PAC.<sup>8b</sup> The small observed reaction volume change is potentially explained by the following: (i) the bond length reduction is not isotropic but rather anisotropic which results in only a small reaction volume change; (ii) compensating increases in other bond lengths in the excited state occur such that the ground- and excited-state volumes are similar; and (iii) the surrounding water molecules do not fill the void created by the compressed excited state, i.e., the excited state is not significantly hydrated.

In contrast, a large reaction volume decrease is observed by PAC upon excitation of  $\text{Pt}_2(\text{P}_2\text{O}_5\text{H}_2)_4^{4-}$  in the presence of  $\text{Tl}^+$  ions, presumably due to formation of the  $^*\text{Pt}_2\text{Tl}^+$  exciplex.<sup>17</sup> The difference in reaction volumes between the formation of  $^*\text{Pt}_2$  and  $^*\text{Pt}_2\text{Tl}^+$ ,  $-11.1 \text{ cm}^3 \text{ mol}^{-1}$ , yields the reaction volume for complexation of the  $^*\text{Pt}_2$  state with  $\text{Tl}^+$  ion. Assuming  $\Delta V_{\text{soln}}$  is negligible,<sup>18</sup> a  $\text{Tl-Pt}$  bond length of  $\sim 2.6 \text{ \AA}$  is suggested by molecular mechanics calculations to account for this structural reaction volume decrease.<sup>19</sup> This bond length is similar to that observed for axial substituents in  $\text{Pt(III)-Pt(III)}$  complexes and also is significantly less than the combined van der Waals radii of the two metals,  $3.7 \text{ \AA}$ ,<sup>20</sup> indicating an appreciable interaction between  $^*\text{Pt}_2$  and  $\text{Tl}^+$ .

Reaction volumes for excimer and exciplex formation can also potentially be obtained via pressure measurements.<sup>21</sup> However, this approach is limited in that the excited state and complex must be luminescent, and the requisite analysis involves numerous assumptions. Consequently, PAC provides a simple alternative method for measuring reaction volumes for excited-state complexation in cases where pressure studies may or may not be possible. In this regard, PAC may be particularly well-suited for the detection of triplet exciplexes, where often only indirect measures of their properties are available.

In conclusion, PAC yields reaction enthalpy, reaction volume, and potentially kinetic information about photoprocesses involving both luminescent and nonluminescent short-lived excited states. The reaction volume data can be related to structural changes in the excited state which may provide insight into excited-state reaction dynamics. Further PAC studies will examine other excited-state complexation processes.

**Acknowledgment.** This work was supported by the National Science Foundation (CHE-8713720), the Research Corporation, and the donors of the Petroleum Research Fund, administered by the American Chemical Society. We thank Prof. Kevin Peters and Dr. Gary Snyder for updated computer programs and D. Pensak for the molecular volume subroutine.

Registry No.  $\text{Pt}_2(\text{P}_2\text{O}_5\text{H}_2)_4^{4-}$ , 85565-26-0;  $\text{TlNO}_3$ , 10102-45-1.

(17) In contrast, the addition of a noncomplexing salt,  $\text{KNO}_3$  (0.02 M), has no effect on the experimental  $\Delta H$  and  $\Delta V_{\text{rx}}$  values.

(18) The magnitude of  $\Delta V_{\text{soln}}$  for exciplex formation is difficult to estimate. The photoprocess involves partial desolvation of both  $\text{Pt}_2$  and the  $\text{Tl}^+$  ion in order to form the complex. Although  $\Delta V_{\text{soln}}$  values for ion pair formation have been measured,<sup>25</sup> none are known for inorganic exciplex formation in water.

(19) Energy minimization of  $\text{Pt}_2(\text{P}_2\text{O}_5\text{H}_2)_4^{4-}$ ,  $^*\text{Pt}_2$ , and  $^*\text{Pt}_2\text{Tl}^+$  structures was done by using MODEL (Version 2.94). The  $\text{Pt-Pt}$  bond length was fixed at 2.92, 2.71, and 2.71 Å for  $\text{Pt}_2(\text{P}_2\text{O}_5\text{H}_2)_4^{4-}$ ,  $^*\text{Pt}_2$ , and  $^*\text{Pt}_2\text{Tl}^+$ , respectively. The volumes of the energy-minimized structures were determined by using an adapted subroutine to the MODEL program.<sup>26</sup> The  $\text{Pt-Tl}$  bond length was fixed at several positions, 2.0–5.0 Å, and the volume of each energy-minimized structure determined.

(20) Bondi, A. J. *Phys. Chem.* **1964**, *68*, 441.

(21) (a) Braun, v. H.; Forster, T. *Ber. Bunsenges. Phys. Chem.* **1966**, *70*, 1091. (b) Pollmann, P.; Rehm, D.; Weller, A. *Ber. Bunsenges. Phys. Chem.* **1975**, *79*, 692. (c) Pollmann, P.; Weller, A. *Ber. Bunsenges. Phys. Chem.* **1973**, *77*, 1071. (d) Seidel, H. P.; Selinger, Aust. *J. Chem.* **1965**, *18*, 977.

(22) Alexander, K. A.; Bryan, S. A.; Dickson, M. K.; Hedden, D.; Roundhill, D. M. *Inorg. Synth.* **1986**, *26*, 211.

(23) Riddick, J. A.; Bunger, W. B.; Sankano, T. K. *Organic Solvents, Physical Properties and Methods of Purification*; Wiley: New York, 1986; Vol. 2.

(24) Weller, A. *Z. Phys. Chem. Neue Folge* **1982**, *93*, 133.

(25) Marcus, Y. *Ion Solvation*; Wiley: New York, 1985; pp 218–230.

(26) Pensak, D. *Ind. Res. Dev.* **1983**, *25*, 74.

## The Solvent Effect on the Electronic Nature of 1,3-Dipoles: An ab Initio SCRF Study

Thomas Steinke,<sup>1</sup> Elke Hänsele, and Timothy Clark\*

Institut für Organische Chemie der  
Friedrich-Alexander-Universität Erlangen-Nürnberg  
Henkestrasse 42, D-8520 Erlangen  
Federal Republic of Germany

Received April 17, 1989

The controversy about the electronic nature of 1,3-dipoles<sup>2</sup> has received much attention, both experimental and theoretical,<sup>3</sup> over the last two decades. Recently, Kahn, Hehre, and Pople<sup>4</sup> used ab initio molecular orbital theory in a novel way to investigate a series of 22- and 24-electron 1,3-dipoles. They used the difference between the restricted Hartree-Fock (RHF) and unrestricted Hartree-Fock (UHF) total energies for a given molecule as a measure of the degree of diradical character. Recent advances in the molecular orbital theory of macroscopic solvent effects suggested that it should now be feasible to investigate the solvent effect on the electronic nature of 1,3-dipoles by combining the self-consistent reaction field (SCRF) approach<sup>5-7</sup> with Hehre and Pople's UHF/RHF criterion to gain some insight into the nature of 1,3-dipoles in solution. We now report results for a series of 24-electron 1,3-dipoles in three solvents, *n*-hexane, methanol, and water. Since Kahn, Hehre, and Pople found no RHF → UHF instability for 22-electron 1,3-dipoles, these were not included in this study.

The 6-31G\*<sup>8</sup> basis set was used throughout, and the geometries used for the "solution" calculations were those obtained by optimization at RHF/6-31G\* or UHF/6-31G\* in vacuo.<sup>4</sup> Table I shows the energy differences between the UHF and RHF calculations. The fact that the UHF wave functions do not collapse to RHF when the latter is more stable is surprising as the RHF solution must also be the true UHF solution. Geometry effects

(1) Permanent address: Humboldt Universität zu Berlin, Sektion Chemie, Bunsenstrasse 1, 1040 Berlin, German Democratic Republic.

(2) See, for instance: Huisgen, R. In *1,3-Dipolar Cycloaddition Chemistry*; Padwa, A., Ed.; Wiley: New York, 1984; Vol. 1, p 1.

(3) See, for instance: Houk, K. N.; Yamaguchi, K. In *1,3-Dipolar Cycloaddition Chemistry*; Padwa, A., Ed.; Wiley: New York, 1985; Vol. 2, p 407.

(4) Kahn, S. D.; Hehre, W. J.; Pople, J. A. *J. Am. Chem. Soc.* **1987**, *109*, 1871.

(5) See, for instance: Rivail, J. L.; Rinaldi, D. *Chem. Phys.* **1976**, *18*, 233. Rinaldi, D.; Ruiz-Lopez, M. F.; Rivail, J. L. *J. Chem. Phys.* **1983**, *78*, 834. Rivail, J. L.; Terryn, B.; Rinaldi, D.; Ruiz-Lopez, M. F. *THEOCHEM* **1985**, *120*, 387. Tapia, O.; Sussman, F.; Poulain, E. *J. Theor. Biol.* **1978**, *71*, 49. Tapia, O.; Constancell, R. *Theor. Chim. Acta* **1978**, *48*, 75. McCreery, J. H.; Christoffersen, R. E.; Hall, G. C. *J. Am. Chem. Soc.* **1976**, *98*, 7191.

(6) Pascual-Ahuir, J. L.; Tomasi, J.; Bonaccorsi, R. *J. Comput. Chem.* **1987**, *8*, 778. Miertus, S.; Scrocco, E.; Tomasi, J. *Chem. Phys.* **1981**, *55*, 117. Bonaccorsi, R.; Cimraglia, R.; Tomasi, J. *J. Comput. Chem.* **1983**, *4*, 567.

(7) Tomasi's SCRF procedure using spherical cavities around the atoms<sup>6</sup> was installed in the Convex version of Gaussian 82 (Binkley, J. S.; Whiteside, R. A.; Raghavachari, K.; Seeger, R.; DeFrees, D. J.; Schlegel, H. B.; Frisch, M. J.; Pople, J. A.; Kahn, L. "Gaussian 82"; Carnegie-Mellon University: Pittsburgh, PA, 1982). The SCF/self-polarization iterations were continued until the total energy in the solvent had converged within  $10^{-8}$  hartrees. The dispersion energy was not included in the solvent effect calculations. The sphere radii used for the atoms were 20% larger than the van der Waals radii (hydrogen, 1.44 Å; carbon, 1.92 Å; nitrogen, 1.80 Å; oxygen, 1.68 Å). The solvent effect calculations were carried out at 298.15 K with the following values for the solvent diameter,  $\sigma$  (Å); taken from the following: Pierotti, R. A. *Chem. Rev.* **1976**, *76*, 17) and for the density,  $d$  (g/cm<sup>3</sup>), thermal expansion coefficient,  $\alpha$ , and dielectric constant,  $\epsilon$  (all taken from the following: Riddick, J. A.; Bunger, W. B.; Sahano, T. K. *Organic Solvents*; Wiley: New York 1986; Vol. 2). The total energies in solution given below include the electrostatic interaction energy and the cavity energy.

solvent	$\sigma$	$d$	$\alpha$	$\epsilon$
<i>n</i> -hexane	5.94	0.65484	0.001391	1.8799
methanol	3.71	0.78637	0.001196	32.66
water	2.77	0.99705	0.000257	78.36

(8) Hariharan, P. C.; Pople, J. A. *Theor. Chim. Acta* **1973**, *28*, 213. Francl, M. M.; Pietro, W. J.; Hehre, W. J.; Binkley, J. S.; Pople, J. A. *J. Chem. Phys.* **1982**, *77*, 3654.

**Table I.** Calculated Relative Energies ( $\Delta E = (E_{\text{RHF}} - E_{\text{UHF}})/\text{kcal mol}^{-1}$ ) Values for Some 24-Electron 1,3-Dipoles<sup>a</sup>

species <sup>b</sup>	vacuum	n-hexane	methanol	water
CH <sub>2</sub> NHO	6.1	0.7	-6.0	-6.3
CH <sub>2</sub> NHNNH	11.2	7.4	0.5	0.2
CH <sub>2</sub> ONH	28.7	16.5	-3.9	-4.8
CH <sub>2</sub> OO	8.7	-8.0	-35.3	-38.0
HNOO	38.4	28.7	10.4	9.4
NHONH	42.7	42.8	43.1	43.1
O <sub>3</sub>	47.8	46.1	43.6	43.5

<sup>a</sup>The sign convention conforms to that used in ref 4 (positive  $\Delta E$  corresponds to a more stable UHF wave function). <sup>b</sup>The conformations and symmetry constraints used correspond to those in ref 4.

are significant in this respect. UHF/SCRF calculations at the RHF-optimized geometries converge to a wave function close to, but not identical with, the RHF solution. The UHF/SCRF calculations do, however, always converge to the same wave function if an unsymmetrical initial guess is used, even if the initial reaction field is that obtained from a RHF calculation. SCRF optimizations would clearly be desirable, but exceed our present computer capacity.

Molecules with a large permanent dipole moment, such as CH<sub>2</sub>NHO, CH<sub>2</sub>NHNNH, CH<sub>2</sub>ONH, CH<sub>2</sub>O<sub>2</sub>, and NHO<sub>2</sub>, show a consistent trend as the polarity of the solvent increases. The calculated dipole moments in both the UHF and RHF calculations increase rapidly at low values of the dielectric constant,  $\epsilon$ , and level off between methanol ( $\epsilon = 32.7$ ) and water ( $\epsilon = 78.4$ ). The expectation values of ( $S^2$ ) also decrease slightly in the UHF calculations as the solvent polarity is increased. The most significant effect, however, is the preferential stabilization of the more polar RHF structures by the macroscopic solvent effect. According to Hobb's extension<sup>10</sup> of Onsager's reaction field theory,<sup>11</sup> the stabilization experienced by a polarizable dipole in a polar solvent should be proportional to the square of the dipole moment of the dipole for any given solvent. The preferential solvent stabilization of the RHF wave functions should therefore depend on the difference between the squares of the RHF- and UHF-calculated dipole moments for the substrate molecules. Figure 1 shows a plot of  $\Delta\Delta E (= \Delta E_{\text{vacuum}} - \Delta E_{\text{solvent}})$  vs  $\Delta(\mu^2)$ . There is a good linear correlation between the two quantities for each of the solvents, suggesting that a knowledge of  $\Delta E$  and the dipole moments from the in vacuo calculations is enough to be able to estimate  $\Delta E$  in solution. This correlation suggests that the UHF and RHF polarizabilities for the seven molecules are all similar.<sup>10</sup> This may not be the case for larger systems, but this can be tested by using semiempirical SCRF theory. The equations obtained from a least-squares analysis of the three lines are given in the figure caption. The slopes of the lines obtained for the three solvents considered correlate with several of the one-parameter empirical solvent polarity scales,<sup>12</sup> but results for more solvents are needed before any useful correlation can be deduced because of the limited number and poor distribution of the solvents treated here.

In the case of the symmetrical A-B-A species (O<sub>3</sub> and NHONH in Table I), the solvent effect is far smaller than that observed for the A-B-C molecules. There is therefore a fundamental difference between A-B-C molecules, in which the permanent 1,3-dipole moment leads to a strong preferential solvent stabilization of the zwitterionic structure, and the A-B-A species, which have much smaller dipole moments roughly bisecting the A-B-A angle. One particularly interesting example is HNONH, for which the calculated UHF gas-phase dipole moment is *larger* than its RHF equivalent. In this case, a small abnormal preferential stabilization of the UHF wave function is found in solution,

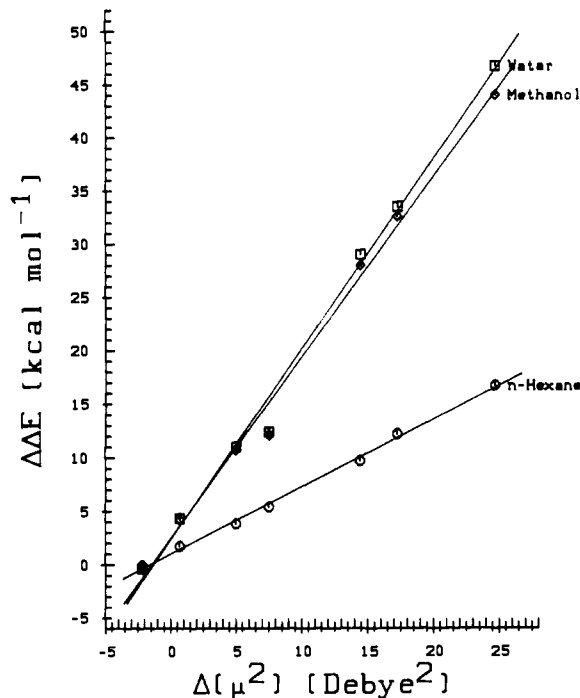
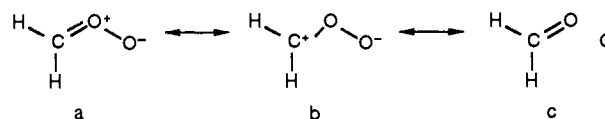


**Figure 1.** The solvent dependency of the energy difference between UHF and RHF calculations for the molecules shown in Table I.  $\Delta(\mu^2)$  and  $\Delta\Delta E$  are defined in the text. The lines are the best least-squares fits. The corresponding equations are  $\Delta\Delta E_{\text{hexane}} = \Delta(\mu^2)(0.63 \pm 0.01) + (1.00 \pm 0.19)$ ,  $\Delta\Delta E_{\text{methanol}} = \Delta(\mu^2)(1.70 \pm 0.06) + (2.44 \pm 0.81)$ , and  $\Delta\Delta E_{\text{water}} = \Delta(\mu^2)(1.78 \pm 0.07) + (2.33 \pm 0.86)$ .

as shown in Table I. The large UHF dipole moment for NHONH is due to the long ON bonds in the UHF-optimized geometry compared to those obtained at RHF. This example shows, however, that the reasonable hypothesis that solvation should always favor the zwitterionic form need not be true.

For the more "normal" molecules, however, a natural bond orbital (NBO)<sup>13</sup> analysis of the vacuum and solution wave functions confirms the preferential stabilization of the zwitterionic forms in solution. The RHF structure for CH<sub>2</sub>OO can be described as a combination of resonance structures a and b with some contribution from the "no bond resonance" structure c. The shifts



observed in the charges and bond orders in going from vacuum to water suggest that resonance form b becomes more important in solution, as might be expected.

**Acknowledgment.** This work was supported by the Deutsche Forschungsgemeinschaft, Fonds der Chemischen Industrie, Stiftung Volkswagenwerk, the Bundesministerium für Innerdeutsche Beziehungen (T.S.), and the Convex Computer GmbH. We especially thank Prof. J. Tomasi and Dr. C. Ghio for providing us with their SCRF program, which was used as a basis for our Gaussian 82/SCRF program, and Prof. J. L. Rivail for useful discussions.

**Registry No.** CH<sub>2</sub>NHO, 75-17-2; CH<sub>2</sub>NHNNH, 107081-72-1; CH<sub>2</sub>O-NH, 62024-17-3; CH<sub>2</sub>OO, 78894-19-6; HNOO, 66619-02-1; NHONH, 66619-03-2; O<sub>3</sub>, 10028-15-6.

(9) Steinke, T.; Clark, T.; Mordí, R. C.; Walton, J. Manuscript in preparation.

(10) Hobbs, M. E. *J. Chem. Phys.* **1939**, *7*, 849.

(11) Onsager, L. *J. Am. Chem. Soc.* **1936**, *58*, 1486.

(12) For leading references, see, for instance: Buncel, E.; Srinivasan, R. *J. Org. Chem.* **1989**, *54*, 798. Abraham, M. H.; Grellier, P. L.; Abboud, J.-L. M.; Taft, R. W. *Can. J. Chem.* **1988**, *66*, 2673.

(13) Foster, J. P.; Weinhold, F. *J. Am. Chem. Soc.* **1980**, *102*, 7211. Reed, A. E.; Weinstock, R. B.; Weinhold, F. *J. Chem. Phys.* **1985**, *83*, 735-746. Reed, A. E.; Weinhold, F. *J. Chem. Phys.* **1985**, *83*, 1736-1740. Reed, A. E. Ph.D. Dissertation, University of Wisconsin-Madison, 1985; *Diss. Abstr. Int.* **1986**, *46*, 4259B. Reed, A. E.; Weinhold, F. *Quant. Chem. Prog. Exch. Bull.* **1985**, *5*, 141-142. Reed, A. E.; Weinhold, F.; Curtiss, L. A. *Chem. Rev.* **1988**, *88*, 899-926.

**Supplementary Material Available:** A table of the UHF and RHF energies, dipole moments, and  $\langle \hat{S}^2 \rangle$  values for the SCRf calculations (2 pages). Ordering information is given on any current masthead page.

## Antibody-Catalyzed Redox Reaction†

N. Janjić‡ and A. Tramontano\*

Department of Molecular Biology  
Research Institute of Scripps Clinic  
La Jolla, California 92037

Received August 10, 1989

It is now well established that antibodies can attain enzyme-like attributes.<sup>1</sup> Several examples of acyl transfer reactions,<sup>2</sup> a pericyclic reaction,<sup>3</sup> and a  $\beta$ -elimination<sup>4</sup> have been subject to acceleration by antibodies. Other types of reactions, such as oxidation-reduction, are less obvious candidates for antibody catalysis for lack of a general strategy for defining mimics of an activated complex.

A common feature of oxidoreductases is the existence of multiple binding sites for substrates and cofactors. Therefore any attempt to use antibodies as redox catalysts should address the possibility for two or more ligands to simultaneously occupy the combining site. We recently described the multiligand binding properties of anti-fluorescein antibodies.<sup>5</sup> Their affinity for fragments of the hapten is consistent with molecular recognition at adjacent subsites of the combining region. The recognition of various reducible dyes in proximity to a secondary binding site for carboxylates suggested the possibility for redox chemistry between ligands bound at the two subsites. Here we report the catalytic activity of anti-fluorescein antibodies in the reduction of a dye substance, resazurin (1), by sulfite.

The benzoate fragment of fluorescein is rigidly aligned with the xanthenyl fragment through a carbon-carbon bond to the C(9) position. The carboxylate group is oriented above the plane of the tricyclic group and as appropriate for nucleophilic addition or electron transfer to the electrophilic atoms of a xanthene or phenoxazine moiety. Antibodies to a fluorescein hapten may be capable of aligning two substrates in a chemically productive complex (Scheme I). The dye resazurin has been used extensively as a redox indicator,<sup>6</sup> and its analogy with 3,6-dihydroxyxanthenes makes it a good ligand for anti-fluorescein antibodies.

Resazurin is reduced by sulfite (or bisulfite)<sup>7</sup> to produce re-

† This is Contribution 6011-MB from the Department of Molecular Biology, Scripps Clinic and Research Foundation, La Jolla, CA 92037.

‡ Cancer Research Institute Postdoctoral Fellow.

(1) Jencks, W. P. *Catalysis in Chemistry and Enzymology*; McGraw-Hill: New York, 1969; p 288.

(2) Tramontano, A.; Janda, K. D.; Lerner, R. A. *Science (Washington, D.C.)* **1986**, *234*, 1566. Pollack, S. J.; Jacobs, J. W.; Schultz, P. G. *Science (Washington, D.C.)* **1986**, *234*, 1570. Napper, A.; Benkovic, S. J.; Tramontano, A.; Lerner, R. A. *Science (Washington, D.C.)* **1987**, *237*, 1041. Jacobs, J. W.; Schultz, P. G.; Sugawara, R.; Powell, M. J. *Am. Chem. Soc.* **1987**, *109*, 2174. Tramontano, A.; Ammann, A. A.; Lerner, R. A. *J. Am. Chem. Soc.* **1988**, *110*, 2282. Janda, K. D.; Lerner, R. A.; Tramontano, A. *J. Am. Chem. Soc.* **1988**, *110*, 4837. Janda, K. D.; Schloeder, D.; Benkovic, S. J.; Lerner, R. A. *Science (Washington, D.C.)* **1988**, *241*, 1188. Benkovic, S. J.; Napper, A. D.; Lerner, R. A. *Proc. Natl. Acad. Sci. U.S.A.* **1988**, *85*, 5355. Iverson, B. L.; Lerner, R. A. *Science (Washington, D.C.)* **1988**, *243*, 1184. Pollack, S. J.; Hsiun, P.; Schultz, P. G. *J. Am. Chem. Soc.* **1989**, *111*, 5961.

(3) Jackson, D. Y.; Jacobs, J. W.; Sugawara, R.; Reich, S. H.; Bartlett, P. A.; Schultz, P. G. *J. Am. Chem. Soc.* **1988**, *110*, 4841. Hilvert, D.; Carpenter, S. H.; Nared, K. D.; Auditor, M. T. *Proc. Natl. Acad. Sci. U.S.A.* **1988**, *85*, 4953.

(4) Shokat, K. M.; Leumann, C. J.; Sugawara, R.; Schultz, P. G. *Nature (London)* **1989**, *338*, 269.

(5) Janjić, N.; Schloeder, D.; Tramontano, A. *J. Am. Chem. Soc.* **1989**, *111*, 6374.

(6) Twigg, R. S. *Nature (London)* **1945**, *155*, 401. DeBaun, R. M.; Kudzin, S. F.; Schubert, W. J. *Arch. Biochem.* **1950**, *26*, 375.

(7) With a  $pK_a$  of 6.9,  $\text{HSO}_3^-$  is the predominant ionization state in acidic pH.

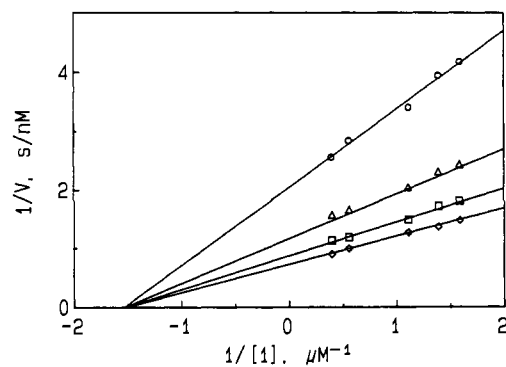


**Figure 1.** Lineweaver-Burk plot for reduction of 1 by 0.5 (O), 1.0 (Δ), 1.5 (□), and 2.0 (◇) mM sulfite catalyzed by monoclonal antibody (MAB) 66D2 at  $1.4 \times 10^{-7}$  M. Initial catalytic rates were determined by measuring the absorbance decrease at 605 nm ( $\epsilon_{605} = 4.3 \times 10^4$  au  $\text{M}^{-1} \text{cm}^{-1}$ ) at pH 5.8 and  $25.0 \pm 0.1$  °C in 10 mM Bis-Tris buffer containing 80  $\mu\text{M}$  EDTA, correcting for the uncatalyzed rate. Linear regression  $y$  intercepts and slopes from this plot were used in secondary plots to determine the values of  $k_{\text{cat}}$ ,  $K_m^S$ , and  $K_m^I$ . These values were used to draw the lines shown.

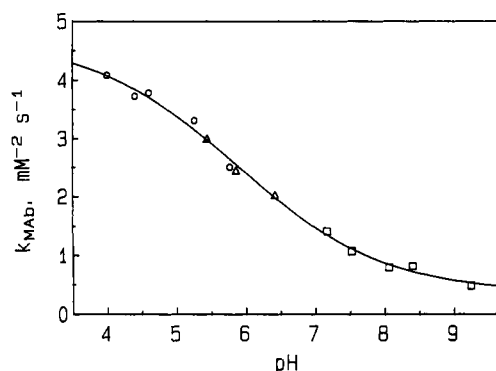
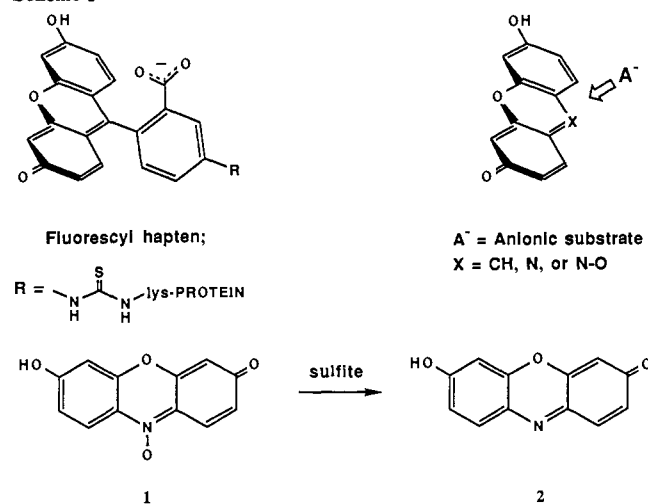


**Figure 2.** The pH dependence of 66D2-catalyzed reduction of 1 (2.6  $\mu\text{M}$ ) with sulfite (1 mM) in 2 mM pyridine (O), Bis-Tris (Δ), and Tris (□) buffers measured as described in Figure 1. First-order dependence in 66D2 allows calculation of  $k_{\text{MAB}}$  from plots of  $k_{\text{obsd}}$  vs [MAB] ( $V_{\text{obsd}} = \{k_{\text{uncat}} + k_{\text{MAB}}[\text{MAB}]\}[\text{sulfite}][\text{I}]$ ).

### Scheme I



sorufin (2) as determined by spectroscopic and chromatographic identification.<sup>8</sup> The reaction rate is first order in each substrate with a second-order rate constant at pH 5.8,  $k_{\text{uncat}} = 0.104 \text{ M}^{-1} \text{ s}^{-1}$ . Linear dependence of  $\log k_{\text{uncat}}$  on pH, increasing with de-

(8) The reaction product has a UV-vis spectrum in alkaline pH ( $\lambda_{\text{max}}$  at 571 nm, shoulder at 535 nm) identical with that of resorufin. The product also coelutes with resorufin by TLC and reversed-phase HPLC (Vydac 201TP54 C-18 column; 1:1 acetonitrile-water).